J Clust Sci (2009) 20:641–649
DOI 10.1007/s10876-009-0267-0

ORIGINAL PAPER

Computer Simulation on TiO_2 Nanostructure Films and Experimental Study Using Sol–Gel Method

E. Zaminpayma · A. Bahramian · M. Kalbasi · H. Erfan Nia

Received: 25 December 2008 / Published online: 3 November 2009

Abstract Molecular dynamics simulation with an experimental work was performed on the TiO_2 nanostructure film. The Morse potential function was used for the interatomic interactions. Then, the equations of motion for molecules and atoms are solved by Verlet algorithm. The effects of deposition rate and the number of TiO_2 molecules were studied for morphology characterization of film surface. In addition, TiO_2 nanostructure film was prepared experimentally with the sol–gel dip-coating method. The results of MD simulations provide a reasonable compatibility with Dektak surface profiler, atomic force microscopy (AFM) and scanning electron microscopy (SEM) images due to the morphology and surface structure of films.

Keywords Nanostructure film · Titanium dioxide · Sol–gel preparation · Computer simulation

Introduction

Titanium dioxide (TiO_2) is an important inorganic material with good physical properties, which make it suitable for various applications. The physical properties of TiO_2 have been extensively investigated over the years mainly due to its potentiality for device applications. It has been used in catalysis [1–4], devices [5],

E. Zaminpayma
Department of Physics and Nanotechnology Research Center, Amirkabir University of Technology, Tehran, Iran

A. Bahramian (✉)
Engineering Faculty, Hamedan University of Technology, Mardom Street, Hamedan, Iran
e-mail: bahramian@aut.ac.ir; alibahramichem@yahoo.com

A. Bahramian · M. Kalbasi · H. Erfan Nia
Department of Chemical Engineering, Amirkabir University of Technology, Hafez Avenue, No. 424, Tehran, Iran

sensors [6, 7], and ceramics [8]. TiO_2 nanostructure films are also often used as various optical coatings for its good transmittance in the visible region, high refractive index and chemical stability [9].

In this paper, TiO_2 nanostructure films are studied from two viewpoints: experimental work (Sol–gel dip-coating method) and computer simulation (Molecular Dynamics approach).

The sol–gel method has some advantages such as controllability, high reliability, reproducibility and wide possibility to vary film properties by changing the composition of the solution [10, 11].

MD simulations have been used to study the impact of single cluster over the solid surface. MD simulations of materials applications at the atomic level are becoming an important technique for investigating the configuration of crystals and liquids, melting and crystallization phenomena, phase transitions, diffusion, conductivity, and thermodynamic properties of inorganic materials [12–14]. The method is conceptionally simple; an arbitrary assemblage of N atoms or ions confined to a specific region of space was considered. Generally, several hundreds or thousands of atoms are used. The periodic boundary conditions were applied to generate an infinite system. The particles are given some initial positions and velocities. Time development of the system was then solved by means of the classical Newtonian equations of motion for each time step of 10^{-16}–10^{-14} s.

There are several studies on MD simulations of TiO_2 crystals structural and physical properties. Matsui and Akaogi [15] carried out MD simulations to reproduce the structure and the physical properties of TiO_2 polymorphs. The interatomic potential function used in their work was composed of Coulomb, Van der Waals and Gilbert-type repulsion terms [16]. They reported on reproducing or predicting a wide range of TiO_2 polymorphs properties. Fukuda et. al. [17] performed MD simulations of rutile using the Morse potential [18] instead of the Van der Waals interaction. The Morse potential becomes important when covalent systems are studied.

In this paper, we report the results of MD simulations on TiO_2 nanostructure films by using Morse interatomic potential function and parameters. It is shown that the results of MD simulations provide a good compatible with atomic force microscopy (AFM) and scanning electron microscopy (SEM) images due to morphology and surface structure of films, respectively.

Experimental Procedure

TiO_2 nanostructure films were prepared by the hydrolysis of titaniumtetra-isopropoxide (TTIP) (Aldrich, 99.99%), which is generally used for TiO_2 nanostructure films or TiO_2 nanoparticles by the sol–gel method. The chemical composition of the sol matrix was: $TTIP/EtOH/H_2O/HNO_3$ with 1:10:18:0.1 in molar ratio. The sol matrix was prepared at room temperature by mixing TTIP with absolute ethanol (Aldrich, 99.9%) and nitric acid (Aldrich, 99.9%) as a catalyst. More details of the sol preparation and their characterization can be found in our last papers [19, 20]. TiO_2 thin films were dip-coated on soda lime glass (75 × 25 mm).

The substrates were carefully cleaned; then samples were dried using a hot air blower. Before being deposited, the substrates were heated at 300 °C for an hour and cooled. The TiO_2 thin films formed on the substrates were prepared from the above TiO_2 solution by dip-coating method. The withdrawal speed was 3.5×10^{-3} m s^{-1}. The thickness of the TiO_2 thin films were adjusted by repeating the cycle from dipping to heat treatment at 500 °C using an electric oven for 1 h. The surface morphology was characterized by AFM (DME DS-95-50) and SEM (Cam Scan MV2300); the film thickness was measured using Dektak surface profiler (Talystep IIA)

Inter-atomic Potential Function

In order to describe the inter-atomic interactions of TiO_2 nanostructure films, Morse potential function has been used. This potential was proposed by Morse in 1929 in order to evaluate the vibrational energy levels of diatomic molecules [21]. The Morse potential consists of two exponential terms as follows:

$$u(r_{ij}) = D\{\exp[-2\alpha(r_{ij} - r_0)] - 2\exp[-\alpha(r_{ij} - r_0)]\}\ r_{ij} < r_C \quad (1)$$

where D, r_0, and α are the adjustable parameters of the Morse potential. D (eV) is generally related to the bond strength, r_0 (Å) is the equilibrium interatomic separation, α (Å^{-1}) is related to the curvature at the potential minimum, and r_C is the cut-off distance.

The Morse potential parameters [22] for the Ti–O, Ti–Ti, and O–O interactions are represented in Table 1. Although no constraints were placed on the parameters, they demonstrate physically sensible trends. For instance, the Ti–O interaction has the largest dissociation energy and curvature, while Ti–Ti has the weakest with the longest equilibrium distance.

Molecular Dynamics Simulation

MD simulations have been used to study the TiO_2 nanostructure film over a solid surface. In the MD simulations, an effective code LAMMPS was used which stood for a massively parallel and large scale atomic/molecular simulator, written by Sandia National Laboratories. LAMMPS integrates Newton's equations of motion for collecting atoms, molecules, or macroscopic particles that interact via short- or long-range forces with a variety of initial and/or boundary conditions. In present simulation, the Verlet algorithm [23] was used for the motion of atoms. Ti–O atoms

Table 1 The Morse potential parameters [22] for Ti–O, Ti–Ti, and O–O interactions

Interaction	D (eV)	α (Å^{-1})	r (Å)
Ti–O	1.0279493	3.640737	1.88265
Ti–Ti	0.00567139	1.5543	4.18784
O–O	0.042117	1.1861	3.70366

were located about 20 Å average distances from substrate in the simulation space. The simulation time was 5 ns with 1 ps time step. At first, TiO_2 molecules were moved towards the surface with 1×10^{-4}, 5×10^{-4}, and 1×10^{-3} Å/ns velocity. In this paper the velocity of TiO_2 molecules in simulation equal to deposition rate in dip-coating method was considered. The MD simulations in this work were fully dynamical and two-dimensional calculations. The results of simulation were obtained for TiO_2 molecules numbers 500, 1000, and 5000.

Results and Discussions

Figure 1a–c represents the results of simulation for interaction of 500 TiO_2 molecules after 5 ns and deposition rate of 1×10^{-4}, 5×10^{-4}, and 1×10^{-3} Å/ns. It is noted that there are significant morphological differences between Fig. 1a and c.

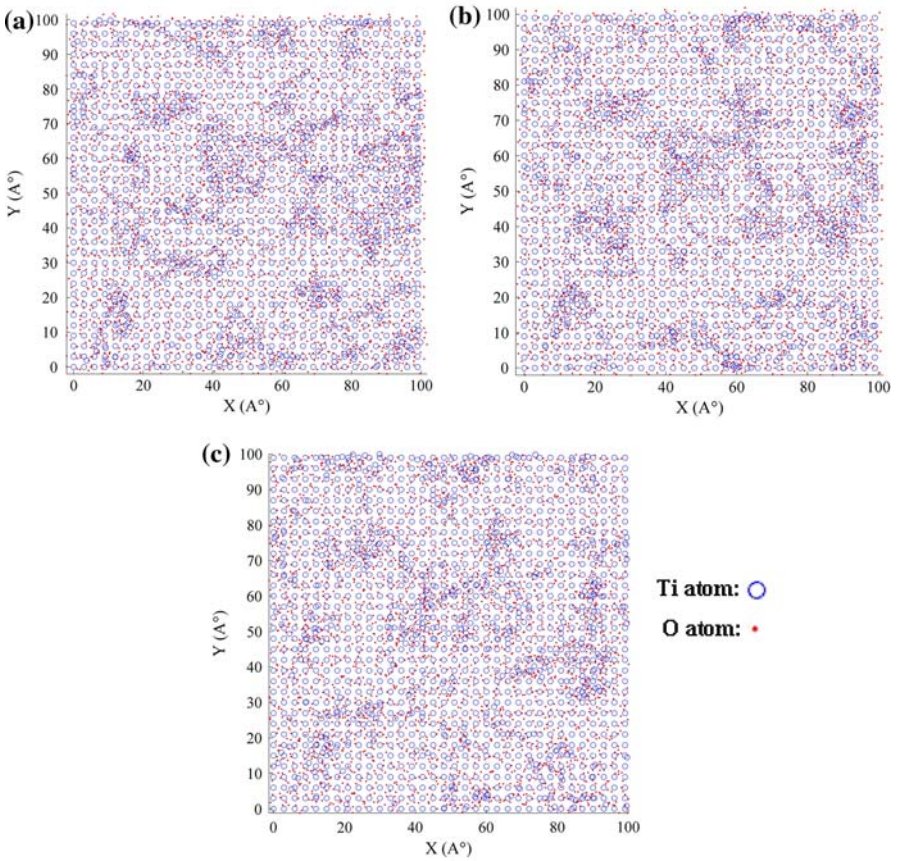

Fig. 1 Interaction of TiO_2–TiO_2 molecules (500 molecules) after 5 ns. Simulation velocity: **a** 1×10^{-4}, **b** 5×10^{-4} and **c** 1×10^{-3} Å/ns

It was shown from this images, clusters and gel structure, Ti–O bonds attached to bridging oxygen and denoted monomers lines and crosses, respectively. The corresponding images were mainly branched clusters. The rapid cluster growth took place through the aggregation of such small clusters. The morphology demonstrated that vacancies and voids were formed within the film, when the number of TiO_2 molecules was 500 (Fig. 1). In Figs. 2 and 3, the number of TiO_2 molecules was 1000 and 5000, respectively. The simulation results of Figs. 2a–c and 3a–c were the same as Fig. 1. In addition, it was found from these images that, when the number of TiO_2 molecules increased, it was due to cluster–cluster aggregation and the network structure of films became dense and packed with TiO_2 molecules.

Our previous experimental studies [20] showed that the deposition rate played a major role in structural properties of films such as film thickness. Figure 4 illustrates surface profile view of 5000 molecules at deposition rate of 1×10^{-4}, 5×10^{-4} and 1×10^{-3} Å/ns. In the MD simulations with increase of deposition rate from 1×10^{-4} to 1×10^{-3} Å/ns, the thickness of film increased from about 23 nm to about 30 nm for each layer.

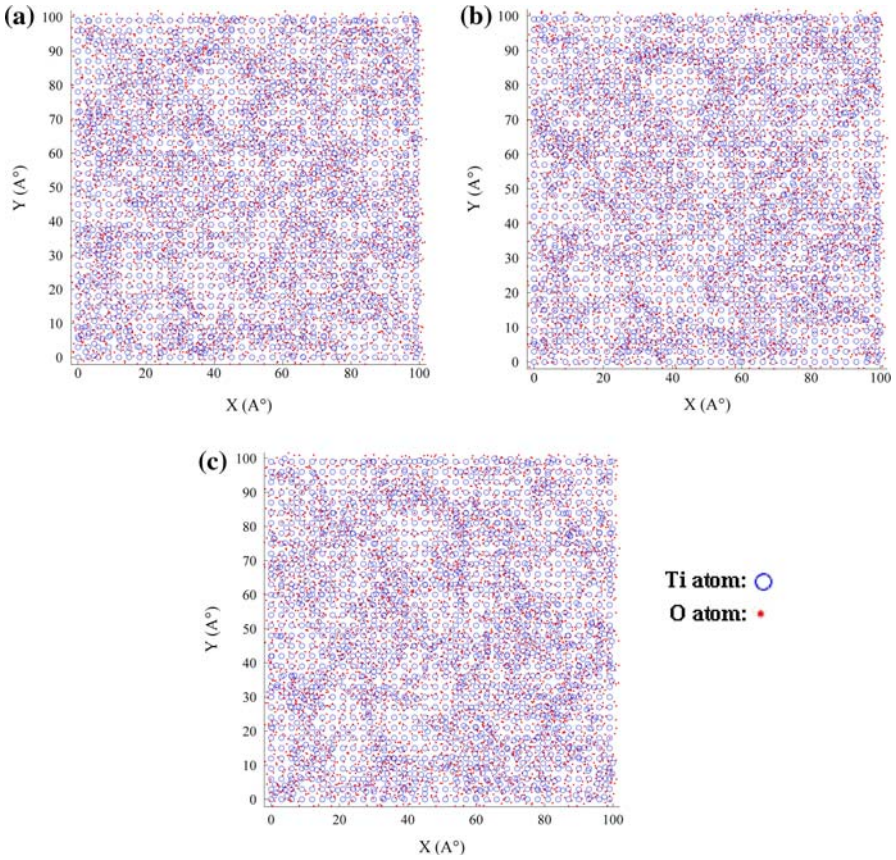

Fig. 2 Interaction of TiO_2–TiO_2 molecules (1000 molecules) after 5 ns. Simulation velocity: **a** $1 \times 10^{-}$, **b** $5 \times 10^{-}$ and **c** 1×10^{-3} Å/ns

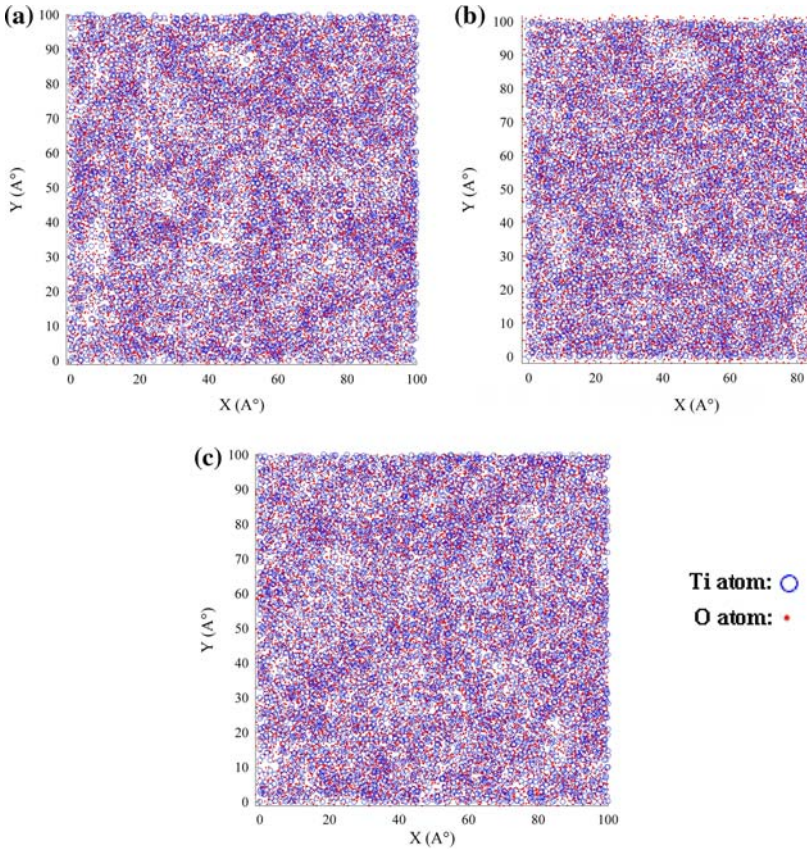

Fig. 3 Interaction of TiO_2–TiO_2 molecules (5000 molecules) after 5 ns. Simulation velocity: **a** 1×10^{-4}, **b** 5×10^{-4} and **c** 1×10^{-3} Å/ns

With observing of the surface profile, it was found that at the lower deposition rates (Fig. 4a), the probability of local clustering in free space was small; thus provided an insufficient number of atoms to yield a uniformly packed film. At the higher deposition rate (Fig. 4c); the local clustering of the incident atoms took place in free space to yield a varied film. Also, when deposition rate increased from 1×10^{-4} Å/ns (Fig. 4a) to 1×10^{-3} Å/ns (Fig. 4c), the structure of thin film changed from packed film to porous film. In order to validate the molecular dynamics simulation, an experimental study on TiO_2 nanostructure films was performed.

Figure 5a shows the SEM image of TiO_2 nanostructure film at 550 °C with a deposition rate of 3.5×10^{-3} m s^{-1}. This value was chosen from among the values of deposition rate in computer simulations. (See Figs. 1, 2, 3, 4). There were a few crystals with small size in the films, but the surface was not very even. It was observed in this image that nanoparticles of TiO_2 were spherical in shape with an average grain size of 30 nm. These results can be compared with Fig. 5a.

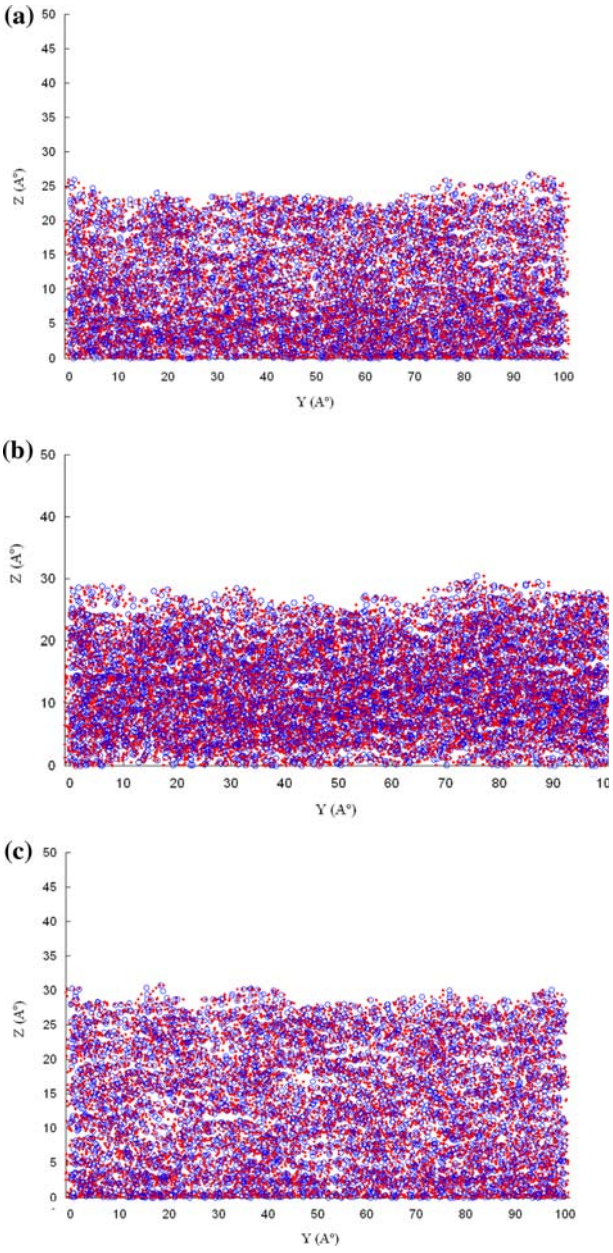

Fig. 4 Surface profile view of 5000 TiO_2 molecules, simulation velocity **a** 1×10^{-4}, **b** 5×10^{-4} and **c** 1×10^{-3} Å/ns

Figure 5b shows the AFM image of uniform agglomeration, small particles and single crystals, were observed and the grains were elongated along the direction of substrate withdrawal from the sol matrix, during the films formation. The dark

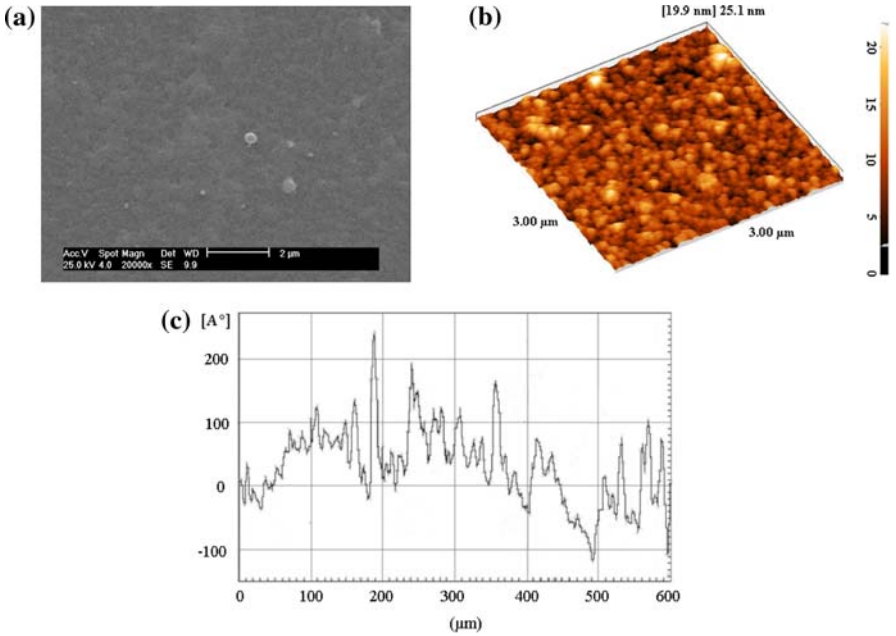

Fig. 5 SEM (**a**) and AFM (**b**) images and Dektak surface profiler (**c**) of TiO_2 nanostructure film surface

groove in the AFM image suggested the appearance of the cracks, but the height profile showed that the deepest section ($\sim$30 nm) was still much smaller than the film thickness ($\sim$240 nm). This suggests that the cracks were superficial. Figure 5c illustrates the surface profile view by Dektak apparatus. It was found from this image that the thickness of the film was varied and the maximum thickness of film was about 24 nm for each layer. The simulated result of Fig. 4 agreed with the film thickness experiment using Dektak apparatus (Fig. 5c).

Conclusion

MD simulations have been employed to study the morphology of the TiO_2 nanostructure films. The Morse potential function was selected to describe the interatomic interactions of TiO_2 molecules and the simulation images showed that the clusters structure was linear and branched. The influence of the number of TiO_2 molecules and deposition rate on film morphology was investigated. At the low deposition rates, uniformly packed film were obtained. When the number of TiO_2 molecules was increased, it was due to cluster–cluster aggregation and network structure of film became dense and packed. Moreover, in this study, the results of MD simulation were compared with the experimental results [20]. Experiments showed that the deposition rate played a major role in structural properties of film such as film thickness. Computer simulations show that with the increase of deposition rate from 1×10^{-4} to 1×10^{-3} Å/ns, the thickness of film increased

from about 23 nm to about 30 nm for each layer and it was in agreement with the deposition dip-coating experiments. The SEM image showed presence of uniform and dense nanostructure with smooth structure and the AFM image revealed the formation of a porous granular surface and small particles, so, the images obtained from computer simulation predicted the experimental results very well.

References

1. N. P. Mellott, C. Durucan, C. G. Pantano, and M. Guglielmi (2006). *Thin Solid Films* **502**, 112.
2. T. Watanabe, A. Nakajima, R. Wang, M. Minabe, S. Koizumi, A. Fujishima, and K. Hashimoto (1999). *Thin Solid Films* **351**, 260.
3. K. Guan (2005). *Surf. Coat. Technol.* **191**, 155.
4. N. Negishi, K. Takeuchi, and T. Ibusuki (1998). *J. Sol–Gel Sci. Technol.* **13**, 691.
5. Q. Fan, B. McQuillin, A. K. Ray, M. L. Turner, and A. B. Seddon (2000). *J. Phys. D Appl. Phys.* **33**, 2683.
6. M. Luo, K. Cheng, W. Weng, C. Song, P. Du, G. Shen, G. Xu, and G. Han (2008). *Mater. Lett.* **62**, 1965.
7. M. Fleisher and H. Meixner (1991). *Sens. Actuators* **B4**, 437.
8. A. C. Pierre (1991). *Ceram. Bull.* **70**, 1281.
9. V. Romeas, P. Pichat, C. Guillard, T. Chopin, and C. Lehaut (1999). *Ind. Eng. Chem. Res.* **38**, 3878.
10. P. Chrysiocopoulou, D. Davazoglou, C. Trapalis, and G. Kordas (1998). *Thin Solid Films* **323**, 188.
11. N. Venkatachalam, M. Palanichamy, and V. Murugesan (2007). *J. Mater. Chem. Phys.* **104**, 454.
12. D. -W. Kim, N. Enomoto, and Z. -E. Nakagawa (1996). *J. Am. Ceram. Soc.* **79**, 1095.
13. D. Terentyev, C. Lagerstedt, P. Olsson, K. Nordlund, J. Wallenius, C. S. Becquart, and L. Malerba (2006). *J. Nucl. Mater.* **351**, 65.
14. E. Salonen, K. Nordlund, J. Keinonen, and C. H. Wu (2003). *J. Nucl. Mater.* **313**, 404.
15. M. Matsui and M. Akaogi (1991). *J. Mol. Simul.* **6**, 239.
16. T. L. Gilbert (1968). *J. Chem. Phys.* **49**, 2640.
17. K. Fukuda, I. Fuji, and R. Kitoh (1993). *Acta Crystallogr.* **849**, 781.
18. P. M. Morse (1929). *Phys. Rev.* **34**, 57.
19. M. Sasani gamsari, A. Bahramian, *13th National Conference on Physics*, 26-31 August, Shahrod, Iran, 2006.
20. M. Sasani Gamsari and A. Bahramian (2008). *Mater. Lett.* **62**, 361.
21. J. P. Rino and N. Studart (1999). *Phys. Rev. B* **59**, 6643.
22. V. Swamy and J. D. Gale (2000). *Phys. Rev. B* **62**, 5406.
23. A. J. Markworth (1984). *Mater. Lett.* **2**, 333.